Effect of group-delay ripples on dispersion-managed soliton communication systems with chirped fiber gratings

Y. H. C. Kwan and P. K. A. Wai

Department of Electronic and Information Engineering, The Hong Kong Polytechnic University, Hong Kong, China

H. Y. Tam

Department of Electrical Engineering, The Hong Kong Polytechnic University, Hong Kong, China

The effect of group-delay ripples in dispersion-managed soliton communication systems that use chirped fiber gratings for dispersion compensation is studied. Using both a reduced model and direct numerical simulation, we find that dispersion-managed solitons exist even in the presence of large dispersion variation caused by group-delay ripples. The dispersion-managed solitons suppress the growth of intersymbol interference induced by the group-delay ripples. © 2001 Optical Society of America

OCIS codes: 060.0060, 060.5530.

Recently, dispersion management has emerged as an important technology in high-bit-rate long-haul optical soliton communication systems. Dispersion-managed (DM) solitons exhibit many advantages. One of them is their robustness to fluctuations in system parameters such as local dispersion.[1,2] Among the many dispersion-compensation techniques, the use of chirped fiber gratings (CFGs) is particularly effective because of their high figure of merit,[3] capability to compensate for higher-order dispersion, and low insertion loss and the absence of nonlinear effects. It has been shown that solitons exist in DM systems that use CFGs for dispersion compensation.[4]

In real chirped fiber gratings, the group-delay response oscillates as a result of residual multiple reflections owing to imperfections in the manufacturing processes. In linear systems, these group-delay ripples lead to intersymbol interference (ISI) and degrade system performance.[5] The group-delay ripples can degrade the intensity noise reduction provided by the gratings in subcarrier multiplexed systems.[6] The group-delay ripples cause large fluctuations of the lumped grating dispersion as a function of wavelength. For example, the average lumped dispersion of the grating studied in Ref. 5 is ~50 ps^2, whereas the dispersion fluctuation can be as large as 4375 ps^2. In this Letter we investigate the effect of group-delay ripples on two-step DM soliton communication systems that use CFGs for dispersion compensation. We model the group-delay ripples by a sinusoidal function and assume that the reflectivity bandwidth of the gratings is much larger than the signal bandwidth. We find that DM solitons exist even in the presence of the large dispersion variation induced by the group-delay ripples. The formation of DM solitons suppresses the growth of ISI.

The evolution of a pulse propagating in an optical fiber under the influence of Kerr nonlinearity and periodically varying dispersion is given by the nonlinear Schrödinger equation

$$i\,\frac{\partial q}{\partial z} - \frac{\sigma(z)}{2}\,\frac{\partial^2 q}{\partial t^2} + |q|^2 q = 0\,, \tag{1}$$

where $q(z,\,t)$ is the normalized envelope of the electric field and z and t represent the normalized distance and time, respectively. The effects of loss and gain are neglected in this study. Dispersion coefficient $\sigma(z)$ is $d/|\overline{d}|$ for $z \neq (n + 1/2)L$, where n is an integer, d is the group-velocity dispersion coefficient of the fiber, $\overline{d}$ is the average group-velocity dispersion of the map, and L is the map period. The gratings are located at $z = (n + 1/2)L$, and their actions are given by the transfer function $F(\omega)$ such that $\tilde{q}_{\mathrm{out}}(z,\,\omega) = F(\omega)\tilde{q}_{\mathrm{in}}(z,\,\omega)$, where ω is the angular frequency and $\tilde{q}_{\mathrm{in}}$ and $\tilde{q}_{\mathrm{out}}$ are the pulse spectra before and after the gratings, respectively. The filter transfer function is modeled as

$$F(\omega) = \exp\!\left[\,i\,\frac{g}{2}\,\omega^2 - i\,\frac{\Gamma}{T_0{}^2}\cos(\omega T_0 + \theta) + i\,\frac{\Gamma}{T_0{}^2}\,\right], \tag{2}$$

where g is the average lumped dispersion of the grating and $\overline{d} = (dL + g)/L$. The parameters Γ, $2\pi/T_0$, and θ are the amplitude, period, and phase, respectively, of the dispersion ripples. The lumped dispersion of the grating is therefore given by $g + \Gamma\cos(\omega T_0 + \theta)$. Equations (1) and (2) can be solved by the variational method. We choose an ansatz

$$
\begin{aligned}
q(z,\,t) = A\sqrt{\eta}\,\exp\{ &-\eta^2(t - C)^2 \\
&+ i[\beta(t - C)^2 + \Omega(t - C) + (\phi/2)]\}, \tag{3}
\end{aligned}
$$

where η, β, Ω, C, and ϕ depend on z and correspond to the amplitude, the quadratic phase chirp, the center frequency, the center position, and the phase, respectively, of the pulse. Parameter A is the energy enhancement, which is independent of z. The evolution of the amplitude and chirp parameters in the optical fiber is given by the following coupled equations:

$$\frac{d\eta}{dz} = 2\sigma\beta\eta\,,$$

$$\frac{d\beta}{dz} = -2\sigma(\eta^4 - \beta^2) - \frac{A^2}{\sqrt{2}}\,\eta^3\,. \tag{4}$$

The effect of the CFG can also be determined by use of the variational method as

$$\eta_{\text{out}}^2 = \eta_{\text{in}}^2/H(\eta_{\text{in}}, \beta_{\text{in}}),$$
$$\beta_{\text{out}} = [\beta_{\text{in}} - 2\overline{g}(\eta_{\text{in}}^4 + \beta_{\text{in}}^2)]/H(\eta_{\text{in}}, \beta_{\text{in}}),$$
$$H(\eta_{\text{in}}, \beta_{\text{in}}) = 4\overline{g}^2(\eta_{\text{in}}^4 + \beta_{\text{in}}^2) - 4\overline{g}\beta_{\text{in}} + 1, \qquad (5)$$

where x_{in} and x_{out} represent the values of parameter x at the input and the output of the grating. Parameter $\overline{g}$ is given by

$$\overline{g} = g + \Gamma \cos(\psi)\exp\left[-\frac{T_0^2}{2}\left(\eta_{\text{in}}^2 + \frac{\beta_{\text{in}}^2}{\eta_{\text{in}}^2}\right)\right], \qquad (6)$$

where $\psi = (\theta - \Omega T_0)$ is the relative phase between the center frequency of the pulse and the ripples. Equations (5) are identical to those of an ideal grating with $\overline{g}$ as the lumped dispersion. From Eq. (6), the effect of the sinusoidal variation of the group-delay ripples is to modify the average lumped dispersion of the grating from g to $\overline{g}$. Because the bandwidth of the chirped Gaussian pulse ansatz B_{grat} equals $2[2\ln 2(\eta^2 + \beta^2/\eta^2)]^{1/2}$ (FWHM) and the ripple period $P_{\text{rip}} = 2\pi/T_0$, the exponent on the right-hand side of Eq. (6) is equal to $-(\pi^2/4\ln 2)(B_{\text{grat}}/P_{\text{rip}})^2$. When the input pulse's bandwidth is much larger than the ripple period, the input pulse sees many periods of group-delay variation. The effect of the group-delay variation is averaged out, and the contribution of the group-delay variation to the effective grating dispersion is small. When the input pulse's bandwidth is smaller than the ripple period, the contribution of the ripples to the effective grating dispersion is large. The ripples may increase or decrease the average lumped dispersion of the grating, depending on the relative phase ψ between the ripples and the input pulse. The maximum contribution from the ripples to the grating dispersion is $\pm\Gamma$.

From Eqs. (5), the grating will reverse the chirp of the soliton without changing the soliton's amplitude if

$$\beta_{\text{in}} - \overline{g}(\eta_{\text{in}}^4 + \beta_{\text{in}}^2) = 0. \qquad (7)$$

Equation (7) is a transcendental equation that relates the amplitude and the chirp coefficient of the pulse at the input of the grating. Figure 1 plots the solutions of Eq. (7). The normalized average grating dispersion is chosen to be $g = -1$. The thick solid curve gives the phase-reversal condition for an ideal grating, i.e., $\Gamma = 0$, and also for the case $\psi = \pi$. We note that $\beta \leq 0$ (≥ 0) for the phase-reversal curve of an ideal anomalous (normal) CFG. The thin solid curves correspond to the phase-reversal conditions for $\Gamma = 6$. The labels on the solid curves are the values of T_0. $T_0 = 0$ represents ideal gratings with lumped dispersion equal to $g \pm \Gamma \cos(\psi)$.

The thick solid curve divides the amplitude chirp plane into two regions. The thin solid curves in Region I correspond to a phase angle ψ of π, and those in Region II correspond to $\psi = 0$. We observe that for each value of η there are two or more values of β for

phase reversal. In Region I ($\psi = \pi$), the center frequency of the soliton is aligned with one of the minima of the dispersion ripples. The effective grating dispersion is always anomalous, i.e., $\beta \leq 0$, because we have chosen $g < 0$. When T_0 is large, the dispersion varies rapidly in a pulse bandwidth. The pulse sees only the average dispersion value. The phase-reversal curves approach those for an ideal grating. When T_0 decreases, the pulse now sees local variation of the dispersion ripples. The effective grating dispersion becomes more anomalous and approaches that of an ideal grating with lumped dispersion $g - \Gamma$.

In Region II ($\psi = 0$), the center frequency of the pulse is aligned with one of the maxima of the dispersion ripples. The behavior of the phase-reversal curves as a function of T_0 is qualitatively similar to that in Region I. However, parts of the phase-reversal curves are in the upper half-plane. In other words, the grating can behave as a normal or as an anomalous-dispersion grating, depending on the amplitude and the chirp coefficient of the input pulse.

The dashed curve in Fig. 1 is the phase-space trajectory of pulse evolution along the fiber according to Eqs. (4). An initial chirp-free pulse begins at $(\eta, \beta) = (1, 0)$ and moves into the lower half of the amplitude chirp plane as the pulse propagates along the fiber. For a given fiber length and fiber dispersion coefficient, the curve terminates on one of the phase-reversal curves. If a corresponding grating is placed at the end of the fiber, the grating will reverse the chirp coefficient β of the pulse without changing its amplitude. A similar piece of fiber placed after the grating will return the pulse to its initial point in the amplitude chirp plane at the end of the fiber. A periodic orbit is thus formed. Figure 1 shows that DM solitons are possible even if the amplitude of dispersion ripples Γ is much larger than the average grating dispersion. The results are qualitatively the same in the presence of loss.

Although reduced models are quite useful in the study of DM systems, their results are only qualitatively correct. Direct numerical simulations are necessary for determining the periodic DM soliton solutions. We apply a numerical averaging method[7]
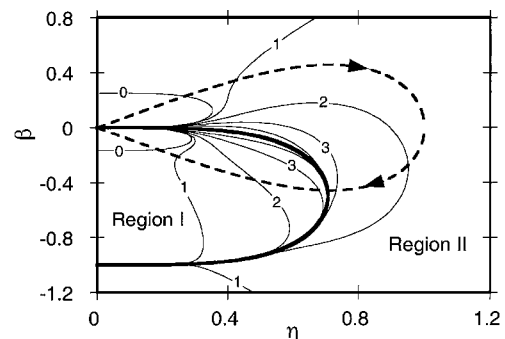

Fig. 1. Phase-reversal curves for chirped fiber gratings with sinusoidal group-delay variation. The average lumped dispersion is $g = -1$. The thick solid curve represents the ideal grating case with $\Gamma = 0$. Solid curves in Region I represent $\Gamma = 6$ and $\psi = \pi$. The solid curves in Region II represent $\Gamma = 6$ and $\psi = 0$. The dashed curve is the phase-space trajectory of pulse evolution along a fiber according to Eqs. (4).
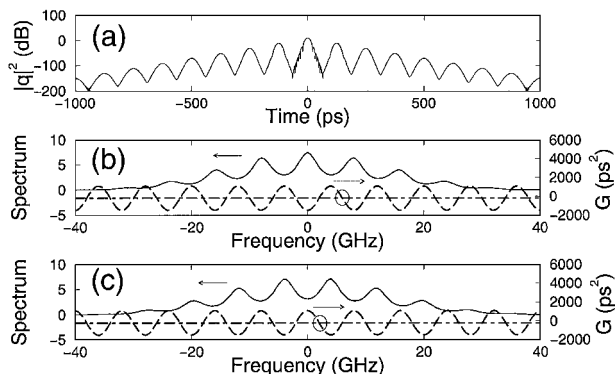
Fig. 2. DM solitons in presence of dispersion ripples: (a) the time intensity profile, (b) the corresponding spectrum, (c) the spectrum of a DM soliton with the same energy but with its center frequency aligned with a dispersion maximum. Parameter G is the lumped dispersion of the grating.

to solve Eqs. (1) and (2). We then propagate the numerical solutions obtained for 100,000 km to determine whether these solutions are true periodic solutions. We find that numerical solutions of the nonlinear Schrödinger equation in general agree with the predictions of the reduced models. If the input pulse's energies are sufficiently large that the bandwidths of the resultant solitons are much larger than the ripple period, the relative phase between the center frequency of the soliton and the ripples does not affect the results. However, when the bandwidths of the solitons are comparable with or less than the ripple period, numerical DM solitons are obtained for $\psi = 0$ and $\psi = \pi$ only. In this case, the center frequency of the DM solitons may be shifted up to one-quarter ripple period from the center of a channel in wavelength-division multiplexing applications. If the soliton bandwidth is comparable with or larger than the ripple period, the time intensity profile of the solitons at the midpoint of the fiber consists of a central Gaussian peak and multiple side peaks. However, if the soliton bandwidth is less than the ripple period, the time intensity profile of the solitons at the midpoint of the fiber consists of a single pulse that resembles a hyperbolic secant.

Figure 2 shows the DM solitons for the following DM system: The map length is 100 km, the average dispersion is -0.1 ps^2/km, the fiber dispersion coefficient is 1.9 ps^2/km, and the average lumped grating dispersion is -200 ps^2. We assume that the amplitude of the group-delay ripples is ~ 10 ps and that the ripple period is 125 ps.[5] The amplitude of the dispersion ripples is therefore 1300 ps^2, or 6.5 times the average lumped dispersion of the grating. Figure 2(a) shows the pulse intensity profile in the time domain taken at the midpoint of the fiber. The soliton consists of a Gaussian-shaped central peak and multiple side peaks located T_0 apart with decreasing amplitude. The FWHM is about 15 ps. Figure 2(b) is the spectrum of the DM soliton shown in Fig. 2(a). The dispersion and the average dispersion

of the grating are shown as a dashed curve and as a dotted–dashed line, respectively. The spectrum also has multiple peaks located at the minima of the dispersion variations where the dispersion is more anomalous. The center of the spectrum is a local maximum because it is aligned with a dispersion minimum, i.e., $\psi = \pi$. Figure 2(c) shows the spectrum of a DM soliton with the same energy but with its center frequency aligned with a maximum of the dispersion variation ($\psi = 0$). The spectrum now has a local minimum at the center. The time intensity profiles for the DM solitons shown in Figs. 2(b) and in Fig. 2(c) are the same. The normalized pulse energy is 12.5. We found that DM solitons also exist if fiber loss is included. Recall that a sinusoidal group-delay variation in CFGs induces ISI because of the formation of multiple side peaks at intervals of T_0.[5] In the absence of a nonlinear effect, the amplitudes of the side peaks increase with the number of gratings that the pulse passes through. In fact, without dispersion, nonlinearity, and loss, the group-delay ripples will redistribute $\sim 30\%$ of the pulse's energy to its side peaks after they pass through 10 of the gratings used in the numerical example. Whereas DM solitons in the presence of group-delay ripples still have side peaks that contribute to ISI, the amplitudes of these side peaks decrease exponentially and do not change as the solitons propagate. For example, the intensity of the first side peaks in Fig. 2(a) is 20 dB less than that of the central peak. Thus DM solitons reduce the effect of ISI induced by the group-delay ripples to a minimum.

In conclusion, we have studied the effect of group-delay ripples in DM soliton communication systems, using CFGs for dispersion compensation. We found that DM solitons exist in the presence of sinusoidal group-delay ripples. The effect of the ripples is to modify the effective lumped dispersion of the grating. The DM solitons suppress the growth of ISI induced by the group-delay ripples in the CFGs.

References

1. T. Hirooka, T. Nakada, and A. Hasegawa, IEEE Photon. Technol. Lett. **12,** 633 (2000).
2. F. Kh. Abdullaev and B. B. Baizakov, Opt. Lett. **25,** 93 (2000).
3. R. Kashyap, in *Fiber Bragg Gratings* (Academic, San Diego, Calif., 1999), Chap. 7.
4. S. K. Turitsyn and V. K. Mezentsev, Opt. Lett. **23,** 600 (1998).
5. S. G. Evangelides, N. S. Bergano, and C. R. Davidson, in *Optical Fiber Communication Conference*, Vol. 4 of 1999 OSA Technical Digest Series (Optical Society of America, Washington, D.C., 1999), p. 5.
6. L. R. Chen, Opt. Commun., **187,** 125 (2001).
7. J. H. B. Nijhof, W. Forysiak, and N. J. Doran, IEEE J. Sel. Top. Quantum Electron. **6,** 330 (2000).